



Published in final edited form as:

Clin Sci (Lond). 2015 October 01; 129(8): 757–767. doi:10.1042/CS20150008.

Substance P enhances microglial density in the substantia nigra through neurokinin-1 receptor/NADPH oxidase-mediated chemotaxis in mice

Qingshan Wang^{*,†}, Esteban Oyarzabal^{*}, Belinda Wilson^{*}, Li Qian^{*}, and Jau-Shyong Hong^{*}

^{*}Neuropharmacology Section, Laboratory of Neurobiology, National Institute of Environmental Health Sciences, Research Triangle Park, NC 27709, USA

[†]Department of Occupational and Environmental Health, School of Public Health, Dalian Medical University, Dalian, Liaoning, 116044, PR China

Abstract

The distribution of microglia varies greatly throughout the brain. The substantia nigra (SN) contains the highest density of microglia among different brain regions. However, the mechanism underlying this uneven distribution remains unclear. Substance P (SP) is a potent proinflammatory neuropeptide with high concentrations in the SN. We recently demonstrated that SP can regulate nigral microglial activity. In the present study, we further investigated the involvement of SP in modulating nigral microglial density in postnatal developing mice. Nigral microglial density was quantified in wild type (WT) and SP-deficient mice from postnatal day 1 (P1) to P30. SP was detected in high levels in the SN as early as P1 and microglial density did not peak until around P30 in WT mice. SP-deficient mice (*TAC1*^{-/-}) had a significant reduction in nigral microglial density. No differences in the ability of microglia to proliferate were observed between *TAC1*^{-/-} and WT mice, suggesting that SP may alter microglial density through chemotactic recruitment. SP was confirmed to dose-dependently attract microglia using a trans-well culture system. Mechanistic studies revealed that both the SP receptor neurokinin-1 receptor (NK1R) and the superoxide-producing enzyme NADPH oxidase (NOX2) were necessary for SP-mediated chemotaxis in microglia. Furthermore, genetic ablation and pharmacological inhibition of NK1R or NOX2 attenuated SP-induced microglial migration. Finally, protein kinase C delta (PKCδ) was recognized to couple SP/NK1R-mediated NOX2 activation. Together, we found that SP partly accounts for the increased density of microglia in the SN through chemotactic recruitment via a novel NK1R-NOX2 axis-mediated pathway.

Keywords

Microglia distribution; chemotaxis; Parkinson's disease

Correspondence should be addressed to Qingshan Wang, M.D, Department of Occupational and Environmental Health, Dalian Medical University, No. 9 Western Section, Lvshun South Street, Dalian, Liaoning 116044, PR China.: wangq4@niehs.nih.gov.

AUTHOR CONTRIBUTION

Qingshan Wang and Jau-Shyong Hong designed the study and wrote the paper; Esteban Oyarzabal wrote the paper; Qingshan Wang, Belinda Wilson and Li Qian performed the experiments; Qingshan Wang analyzed the data.

INTRODUCTION

Microglia are the native innate immune cells of the brain, thus their distribution is thought to be relatively homogenous in uninjured brains to permit more efficient surveillance of brain homeostasis. Yet surprisingly, the distribution of microglia in substantia nigra (SN) is far greater than the surrounding regions; the microglia in the SN of rodents [1, 2] and humans [3] are five and ten-fold denser, respectively, compared to the average density throughout the brain. The putative developmental cues regulating microglial density in the SN still remain unknown.

Recently, neurogenic signals have been shown to modulate microglial activity and function, such as microglial activation, migration, proliferation and phagocytosis [4, 5]. We speculated that substance P (SP), an endogenous neuropeptide expressed in high concentrations in nerve terminals of the striatonigral fibers [6, 7], could be the putative neurogenic signal to regulate microglial density during development. SP is well-known to participate in neuro-immune crosstalk both centrally and peripherally [8]. Within the brain SP mediates various pro-inflammatory responses and is known to play a central role in inflammation-related diseases in the central nervous system [8, 9]. Our recent findings indicate that endogenous SP potentiates lipopolysaccharide (LPS)- and 1-methyl-4-phenyl-1,2,3,6-tetrahydropyridine (MPTP)-induced immunological activation of microglia in the SN, amplifying dopaminergic neurodegeneration in experimental mouse models of PD, suggesting the critical role of substance P in mediating the neuroinflammatory and dopaminergic neurodegeneration [10]. Additionally, SP has previously been shown to attract migrating neurotrophils [11] and monocytes [12]. Together, we hypothesized that SP released from the nerve terminal of striatonigral projections may contribute to the higher microglial densities in the SN through the induction of proliferation and/or through chemotactic recruitment of microglia.

In the present study, we aimed to investigate whether SP could regulate microglial density in the SN by using transgenic mice deficient in endogenous SP (*TAC1*^{-/-}) or the SP receptor (neurokinin-1 receptor, *NK1R*^{-/-}). Since NADPH oxidase (NOX2) mediates the regulatory effects of SP on microglial activity in our previous study [10], NOX2 deficient mice (*gp91^{phox}*^{-/-}, the functional catalytic subunit of NOX2) and derived primary microglia cells were further used to elucidate the potential mechanisms of how SP regulates microglial density.

MATERIALS AND METHODS

Animals

C57BL/6J (WT), *TAC1*^{-/-} (B6.Cg-*Tac1*^{tm1Bbm}/J) and NOX2-deficient mice (*gp91^{phox}*^{-/-}, B6.129S6-Cybbtm1Din/J) were purchased from The Jackson Laboratory (Bar Harbor, Maine, USA). All postnatal mice were euthanized using sodium pentobarbital overdose and cardiac perfusion using 4% paraformaldehyde in PBS. Brains were collected immediately following perfusion fixation. Housing, breeding and experimental use of the animals were performed in strict accordance with the National Institutes of Health guidelines.

Immunohistochemistry and double-labeling immunofluorescence

Fixed mouse brains were processed for immunostaining as described previously [10]. Briefly, after soaking in 4% paraformaldehyde for 2 days of post-fixation, brains were cryoprotected for an additional 2 days in 30% sucrose at 4 °C. Brains were sectioned into 35 µm thick slices containing the SN and were immunoblocked with 4–10% goat serum and then incubated with rabbit polyclonal antibody against SP (1: 16,000) or ionized calcium-binding adaptor molecule 1 (Iba-1, Wako Chemicals, Richmond, VA, USA, 1: 2,000 dilution) for 24h or 48 h at 4°C, respectively. Antibody binding was visualized using a Vectastain ABC Kit and 3,3'-diaminobenzidine. Nigral densities of SP immunostaining were measured using ImageJ [13]. For double-labeling immunofluorescence, brain sections were incubated with 99% formic acid for 5 min for antigen retrieval. After repeated washing with PBS, proliferating microglia in the SN co-stained for antibodies against proliferating cell nuclear antigen (PCNA, 1:200) and Iba-1 (1:2000) were visualized by Alexa-594 (red) and Alexa-488 (green)-conjugated secondary antibodies (1:1000), respectively. After mounting the sections onto glass slides with prolong antifade reagents, fluorescence images were obtained using a Zeiss LSM 510 NLO laser scanning confocal microscope.

Cell counting

The number of Iba-1⁺ cells was counted by a stereological procedure as described previously [14] with minor modifications. The brain regions of interest were outlined under a 10 × objective lenses (captured image area, 65,522 µm²) and the number of Iba-1⁺ cells was estimated using the optical dissection (1 µm per section) method employing a computer-controlled x–y–z motorized stage and 60 × oil immersion objective. The cell counting began 2 µm below the top of the section. The numbers of microglia were counted in the whole selected region. To obtain the density of microglia, the microglia count was divided by the volume (65,522 µm² × 35 µm) of the selected area.

Proliferating microglia were enumerated by double-staining against PCNA and Iba-1 antibodies. The percentage of Iba-1⁺PCNA⁺ cells were calculated with respect to the total number of Iba-1⁺ cells using 3 to 6 visual fields (40 ×) of the SN in all transgenic strains of mice as described previously [15].

Quantification of SP density

The density of SP immunoreactivity was measured using ImageJ software (National Institutes of Health, USA) as described previously [13]. Briefly, nigral pictures with SP staining were taken under a 10 × objective lenses and entire nigral region from each section was selected as the “region of interest (ROI)”. Threshold values for hue (0 – 100), saturation (0 – 255), and brightness (175 – 255) were set in the —Adjust Color Threshold dialog box, and then mean density was measured. Quantification was performed from 3 adjacent brain sections, spaced 120 µm apart, and subsequently averaged for each animal. The background of nonspecific staining with SP antibody was deducted from time-matched *TACT^{-/-}* mice.

Microglia proliferation assay *in vitro*

Mixed glia cultures containing 20% microglia and 80% astrocyte were prepared according to a previously published protocol [16]. The proliferative capacity of microglia *in vitro* was

measured using BrdU incorporation assay as described previously with minor modifications. Briefly, mixed glia cultures were pre-incubated with BrdU (20 $\mu\text{mol/l}$) for 30 mins and followed by SP (10^{-8} M) or vehicle treatment for additional 72h. Cells were treated with BrdU again before 4h of fixation with 4% PF. Subsequently cells were treated with 2N HCl at 37°C for 30 min and incubated with anti-BrdU (1:500) and anti-Iba-1 (1:2000) antibodies overnight at 4 °C. Proliferated microglia co-stained BrdU and Iba-1 were visualized by Alexa-488 (green) and Alexa-594 (red)-conjugated secondary antibodies (1:1000), respectively. The percentage of Iba-1⁺BrdU⁺ cells was calculated with respect to the total number of Iba-1⁺ cells.

Microglial chemotaxis assay

Microglia-enriched cultures were prepared according to a previously published protocol [17]. Chemotaxis was assessed on enriched microglia using a disposable 96-well cell migration system with 5 μm pore size (the ChemoTx® System, Neuro Prob, Gaithersburg, MD, USA) in accordance to the manufacturer's protocol. Briefly, 5×10^4 microglia in phenol red free MEM medium were added to the upper filter and 0.3 mL MEM with different concentrations of SP was placed to the lower reservoir. After incubating for 4h in 5% CO₂ at 37 °C, the cells remaining on the top of the filter were removed with a cotton swab. Cells that had migrated to the bottom of the filter were detached by incubation with EDTA and subsequent centrifugation at $600 \times g$ for 2 minutes. The migrated cells on the lower reservoir were quantified using CyQUANT® Cell proliferation assay kit (Life Technologies, Grand Island, NY, USA). Chemotaxis was expressed as the number of cells per well or migration index, defined as the number of cells migrating in response to SP divided by the number of migrating cells in a control chamber. In studies investigating the effects of NK1R or NOX2 on SP-induced chemotaxis of microglia, microglia cells were pre-treated with NK1R antagonists CP96,345 or L-703,606 or NOX2 antagonist DPI (10^{-13} M) for 30 minutes prior to assaying chemotaxis.

Measurement of superoxide

The production of superoxide and intracellular reactive oxygen species (iROS) were determined by measuring the superoxide dismutase-inhibitable reduction of 2-(4-Iodophenyl)-3-(4-nitrophenyl)-5-(2,4-disulfophenyl)-2H-tetrazolium (WST-1) as described previously [18, 19].

Statistical analysis

All values are expressed as the mean \pm SEM. The differences among means were analyzed using one- or two-way ANOVA with treatment or genotype as the independent factors. When the ANOVA showed significant differences, pair-wise comparisons between means were analyzed by Tukey's *post hoc* testing. The regression analysis was performed by Prism 5.0 using the function of "linear regression". In all analyses, a value of $p < 0.05$ was considered significant.

RESULTS

Mice show correlative increases in SP expression and microglial density in the SN during early postnatal development

The expression of SP in the SN increased gradually from P1 to P30, remaining distinctly higher than the adjacent area—where SP immunostaining was negligible—beginning as early as P1 (Figure 1A). Densitometric analysis showed that immunohistochemical expression of SP was 2.1, 3.9, 4.5 and 5.4 fold greater in the SN in P1, P7, P14 and P30 mice, respectively, when compared to the adjacent region (Figure 1B and D). Coincidentally, the number of microglia in the SN increased gradual throughout the same developmental period as shown through the longitudinal increase of Iba-1⁺ cells in the SN. However, unlike the expression of SP, microglial densities in the SN were not significantly different from the adjacent region until P7. Microglial numbers continued to increase up until the study endpoint of P30 (Figure 1A and C), where microglia found in 2.4 times greater numbers than in the adjacent region (Figure 1D).

A linear regression analysis was performed to determine the existence of an interaction between the gradual increase in SP expression and microglial density in the SN during postnatal development. SP expression and microglial density were positively correlated in the developing SN ($r = 0.9313$, $p < 0.0001$; Figure 1E).

Absence of endogenous SP or NK1R limits microglial accumulation in the developing SN

TAC1^{-/-} mice had a significant reduction in the number of Iba-1⁺ microglia in the SN beginning at P7 through P30 compared to WT controls. Stereological counts revealed *TAC1*^{-/-} mice had 25%, 19% and 20% less nigral microglia at P7, P14 and P30, respectively (Figure 2A). The reduction in the number of microglia within the SN in *TAC1*^{-/-} mice was still observed in 24 month-old mice (**data not shown**). Evaluation of an adjacent area, known to contain very little levels of SP, remained unchanged in *TAC1*^{-/-} mice (Figure 2B) compared to WT controls.

To determine whether SP mediates its effect on microglial density in the SN through its canonical receptor NK1, *NK1R*^{-/-} mice were assessed. *NK1R*^{-/-} mice had reduced numbers of microglia in the SN at P7 and P14 but not at P30. Stereological counts showed 22% and 24% less microglia in the SN of P7 and P14 *NK1R*^{-/-} mice, respectively, compared to WT mice (Figure 2C).

SP fails to modify microglial proliferation

At P7, a robust number of PCNA⁺Iba1⁺ cells were observed in the SN of both WT and *TAC1*^{-/-} mice (Figure 3A), of which there was no difference the rate of microglia undergoing proliferation (Iba-1⁺PCNA⁺/Iba-1⁺) (Figure 3B). Similar findings were observed when Iba1⁺ cells were stained against the proliferative marker Ki67, another marker for proliferating cells (**data not shown**). To further verify no effects of SP on microglial proliferative capacity, mixed glia cultures containing 20% microglia and 80% astrocyte were incubated with BrdU and followed by treatment with exogenous SP (10⁻⁸ M). Proliferated microglia were recognized by double BrdU and Iba-1 immunoreactive cells. Consistent with

in vivo, no difference of microglial proliferative rate (Iba-1⁺BrdU⁺/Iba-1⁺) was found between SP and vehicle-treated cultures (Figure 3C and D).

SP induces microglial migration through a NK1R-dependent manner

In a trans-well migration plate with microglia on the filter and different concentrations of SP in the below media, SP dose-dependently increased the number of microglia that traveled through the filter (Figure 4A), indicating that SP is a chemoattractant to microglia. SP at 10⁻⁸ M concentrations showed the highest chemoattraction towards microglial showing a ~2.6-fold elevation in the number of microglia in the bottom well compared to vehicle control.

NK1R antagonists CP96,345 or L-703,606 were subsequently used to determine whether the NK1R was required for SP-induced microglial chemotaxis. As seen in Figure 4B, both CP96,345 and L-703,606 effectively reduced the number of microglia migrating toward the bottom wells that contained 10⁻⁸ M SP to levels similar to those of untreated controls, indicating that NK1R is critical for SP-induced microglial chemotaxis. These findings were further supported by the failure of SP to induce migration from primary microglia extracted from NK1R^{-/-} mice (Figure 4C).

NOX2-generated superoxide is a critical mediator in SP-induced microglial chemotaxis

To uncover the signaling pathway mediating the SP-NK1R-induced chemotaxis of microglia, we investigated the role of NOX2-generated superoxide. We first determined whether SP could induce microglial production of superoxide by NOX2. SP at 10⁻⁷ and 10⁻⁸ M increased the production of superoxide in mixed glia cultures from WT mice (Figure 5A), yet mixed glia cultures prepared from mice deficient in gp91^{phox}—the catalytic subunit of NOX2—failed to produce superoxide in response to SP stimulation (Figure 5B). Although our primary mixed glia culture consists of both microglia (20%) and astroglia (80%), an earlier report from our laboratory indicates that the primary source of extracellular superoxide is microglial NOX2 [20]. To determine whether NOX2-generated superoxide is required for SP-induced microglial chemotaxis, we evaluated whether the chemoattraction towards SP in primary microglia from WT mice could be pharmacologically suppressed using diphenyleneiodonium (DPI). We found that microglia pretreated with 10⁻¹³ M of DPI—that found to be highly specific for NOX2 both *in vitro* and *in vivo* [21]—significantly reduced chemoattraction of microglia towards SP (Figure 5C). Consistently, microglia prepared from gp91^{phox}^{-/-} mice also failed to migrate towards SP.

NK1R signals the activation of NOX2 in microglia through PKC δ

NK1R antagonists CP96,345 or L-703,606 were used to determine whether SP-induced NOX2 activation was mediated through NK1R signaling. CP96,345 and L-703,606 were both sufficient to effectively attenuate the microglial production of superoxide by SP (Figure 6A). Consistent with this finding, mixed glia cultures from NK1R^{-/-} mice failed to produce superoxide in response to SP stimulation (Figure 6B), indicating that SP-induced NOX2 activation is NK1R dependent.

To evaluate the mechanism by which NK1R signaling induces NOX2 activation in microglia, we evaluated several kinases known to be activated downstream of NK1R including protein kinase A (PKA) and C (PKC) [22, 23]. Interestingly, we found that inhibition of PKC, and not PKA, was sufficient to reduce the production of superoxide elicited by SP (Figure 6C). To further determine the subunit of PKC required to mediate SP-induced NOX2 activation, antagonists for PKC α/β or PKC δ were also assessed. PKC δ , and not PKC α/β , was sufficient to reduce the production of superoxide elicited by SP (Figure 6C).

DISCUSSION

The present study suggested that SP released from striatonigral projections during early postnatal development is partly responsible for the high density of microglia found in the SN by attracting microglia into this region. The salient features of our findings are: 1) the increase of SP density in the SN during postnatal development was earlier than that of microglia and a positive correlation between increases of nigral SP and microglial density was observed; 2) mice deficient in endogenous SP or SP receptor, NK1R displayed reduced microglial density in the SN during postnatal development; 3) SP failed to interfere with microglial proliferative capacity in both *in vivo* and *in vitro*; 4) NK1R or NOX2 knockout abolished SP-induced microglial chemotaxis; 5) PKC δ inhibitor inhibited SP/NK1R-mediated NOX2 activation.

Fate mapping analysis revealed that microglial progenitors originate in the yolk sac and infiltrate the mouse brain around E10.5 [24]. Migration and the subsequent proliferation of these microglial progenitors are essential in giving rise to the population of microglia found throughout the brain [24–26]. Although the neurogenic signal(s) released during early brain development to recruit yolk sac progenitors remain unknown, previous studies have found the neuronal progenitors begin expressing the chemoattractants M-CSF and MIP-2 around the same time microglia progenitors infiltrate the pial surface of the brain [27, 28]. Once microglia have populated the entire brain, M-CSF is released by neuronal progenitors and radial glia to permanently differentiate yolk sac progenitors into microglia [29]. Although very little is known about the neurogenic signals that are involved in the differential concentration of microglia in certain brain regions, a recent study found that mice deficient in IL-34 had reduced microglial numbers in cerebral cortex, corpus callosum, hippocampus and basal ganglia due the regional heterogeneity of these brain regions with regards to IL-34 expression [30]. Our study further extends our knowledge in this field by recognizing SP as a neurogenic regulatory for nigral microglial density. We found that lack of endogenous SP (*TAC1*^{-/-}) reduced the number of Iba-1⁺ microglia in the SN in postnatal development period compared to WT controls. Consistently, SP receptor knockout (*NK1R*^{-/-}) mice also displayed reduced numbers of nigral microglia, although a recovery was observed at P30. One possible explanation for the recovered microglial densities by P30 in *NK1R*^{-/-} mice may be due to the compensatory effects by other tachykinin receptors.

Previous reports show that SP can stimulate the production of the chemokines MIP-2 and MCP-1 in macrophages and neutrophil [31, 32], suggesting that chemotactic effects of SP may be mediated through secondary messengers. MCP-1 is typically produced by astrocytes

and microglia under neuroinflammatory pathologies, resulting in the recruitment and proliferation of additional microglia and infiltrating leukocytes to resolve an insult. Since we have previously shown that SP is pro-inflammatory at concentrations of 10^{-8} M and 10^{-14} M, respectively, signaling microglial activation through NK1R and NOX2 [10], we suspected that SP-activated microglia could recruit other microglia through the release of MCP-1. Interestingly, unlike macrophages and neutrophil, no detectable levels of MCP-1 or MCP-1 transcripts were found in SP-treated primary microglia (data not shown), suggesting that microglial MCP-1 does not mediate SP-induced migration of microglia. Recent findings have shown that MCP-1 is also constitutively released by dopaminergic neurons of the SN in adult rats [33], since neurogenic MCP-1 was not assessed during development, we cannot rule out its possible contribution in the high density of microglia recruited to the SN.

Unlike MCP-1, our study found that SP does not seem to affect the proliferative capacity of microglia but rather serves as a chemoattractant recruiting microglia through a NK1R-dependent manner. No difference of microglial proliferative rate ($Iba-1^{+}PCNA^{+}/Iba-1^{+}$) was observed between WT and *TAC1*^{-/-} mice at P7. The reasons for choosing this time point are: First, microglia keep high proliferative rate (> 50%) [25] and second, a greater difference (about 25%) of nigral microglial density was observed between WT and *TAC1*^{-/-} mice. Consistent with *in vivo*, no difference of microglial proliferative rate ($Iba-1^{+}BrdU^{+}/Iba-1^{+}$) was found between SP and vehicle-treated mixed glia cultures that contain 20% microglia and 80% astrocyte. Purified microglia were not used in this study because they have limited replenishment capacity and become hypersensitive to immune stimuli-induced apoptosis in the condition without the presence of astrocyte [34, 35]. In addition, our pilot study showed that conditioned medium prepared from astrocyte can support the survival of microglia and keep them in ramified morphology (data not shown), which mimic to some degree the condition in brain. In contrast, our dose-response study showed that SP induced microglial migration in a bell curve with peak recruitment at 10^{-8} M concentrations, similar to that of fMLP-induced neutrophil chemotaxis [24]. The exact mechanism by why higher concentrations of SP (10^{-7} – 10^{-6} M) exhibit lower chemotaxis capacity remains unclear. However, a previous report suggests that high concentrations of chemoattractants are poorly efficient at activating p38, a signal pathway that facilitates cell migration, compared with lower chemoattractant concentrations [36]. Surprisingly this dose-response curve is in contrast to the production of NOX2-generated superoxide by SP, whereby high doses (10^{-7} – 10^{-6} M) of SP can still generate superoxide. Although this study found that superoxide was essential for SP-mediated microglial migration, it is interesting to note that it is not sufficient for SP-induced microglial migration. In support of this, we previously reported that a 10^{-13} M concentration of SP activates NOX2 to produce superoxide through an NK1R-independent manner [10], yet we found this concentration failed to induce microglial chemotaxis (Figure 4). Though NOX2 activation has previously been shown to be required for VEGFR1/CSF-1R-mediated chemotaxis [37], our study shows that superoxide alone is not sufficient to drive cell movement. Among these signals we identified the atypical PKC isotype PKC δ as the downstream signal that bridges SP-mediated NK1R activation and NOX2 activation in microglia. Though PKC δ has previously been shown to phosphorylate p47^{phox}, a cytosolic subunit of NOX2, resulting in its membrane translocation required for NOX2 activation [38], this is the first account of PKC δ being involved in chemotaxis.

Our findings suggest that the regionally specific expression of neurogenic SP partly explains why microglia accumulate at higher densities in the SN during postnatal development. Even though some have offered theories as to why dopaminergic neurons of the SN are highly vulnerable to oxidative insults [39], particularly in PD patients and toxin-elicited animal models of PD, the answer to this question remains unanswered. Intrinsic factors such as low buffering capacity against oxidative stress and tonic firing-related increase of dopamine quinones during dopamine catabolism have been offered as potential explanations. We have proposed that the disproportionately high density of microglia in the SN, confirmed in different species [1–3], may also serve as an important extrinsic factor that increases the susceptibility of dopaminergic neurons toxicity in response to cytotoxic neuroinflammatory factors [2]. We previously reported that interactions between dysregulated, overactivated microglia and injured neurons form a self-propelling vicious cycle that causes uncontrolled inflammation and drives progressive collateral dopaminergic neurodegeneration in PD [40]. Additionally, dysregulated SP has been suggested to be involved in PD [41, 42]. Although reduced levels of SP is found in PD patients, the role of SP in the pathogenesis of PD remains controversial. Barker [43] considered that PD may result from a primary loss of active tachykinin, probably SP in the SN and that this loss leads to a secondary degeneration of the dopaminergic neurons. While, Sivam [44] found that the loss of SP is DA-dependent and more than 80% decrease of striatal DA levels is required to deplete SP content. The reason may be due to the stimulatory effects of DA on SP release through binding to its D1 receptor located on striatal SP-containing medium spiny projection neurons [45]. In contrast, in experimental PD models, SP is consistently shown to be toxic to dopaminergic neurons. Mice deficient in endogenous SP displayed more resistance to LPS- and MPTP-induced microglial activation and dopaminergic neurodegeneration in the SN compared with LPS or MPTP-treated WT mice [10]. Thornton and Vink reported that exogenous SP exacerbated microglial activation and dopaminergic degeneration in 6-hydroxydopamine (6-OHDA)-generated mouse PD model, which was further attenuated by treatment with SP receptor antagonists, N-acetyl-L-tryptophan and L-333,060 [46].

In summary, we found that endogenous high levels of SP that accumulate during postnatal development partly account for the subsequent increase in microglial density in the SN. We found that SP mediates microglial increase in density through a novel NK1R-NOX2 axis that recruits migrating microglia. Even though the evidence supporting SP in regulating microglial density in the SN is compelling, it only accounts for 20% to 25% of the increased microglial density in the SN. For this reason we believed other postnatal neurogenic factors such as IL-34, MCP-1, neurokinin A and B and CX3CL1 [47, 48] to be primarily involved in regulating microglial density in the SN. Further investigation of the role of these factors in regulating microglial density in the SN should be conducted. Our study not only recognized SP as a neurogenic signal in regulation of nigral microglial density but also provided valuable insights into the field of how neurogenic signals regulate microglial density in brain. Furthermore, since the disproportionately higher density of microglia and potential SP itself in the SN may contribute to the increased susceptibility of nigral dopaminergic neurons in response to regional neuroinflammation such as that found in PD [2, 49], the development of pharmacological inhibitors of SP/NK1R or NOX2 signals might prove useful to improve the outcome of PD.

Supplementary Material

Refer to Web version on PubMed Central for supplementary material.

Acknowledgments

This research was supported by the Intramural Research Program of the NIH, National Institute of Environmental Health Sciences.

ABBREVIATIONS

DPI	diphenyleiiodonium
Iba-1	ionized calcium-binding adaptor molecule 1
MCP-1	monocyte chemoattractant protein-1
M-CSF	macrophage colony-stimulating factor
MIP-2	macrophage inflammatory protein 2
NK1R	neurokinin-1 receptor
NOX2	NADPH oxidase
PCNA	proliferating cell nuclear antigen
PKA	protein kinase A
PKC	protein kinase C
SN	substantia nigra
SP	substance P

References

1. Lawson LJ, Perry VH, Dri P, Gordon S. Heterogeneity in the distribution and morphology of microglia in the normal adult mouse brain. *Neuroscience*. 1990; 39:151–170. [PubMed: 2089275]
2. Kim WG, Mohny RP, Wilson B, Jeohn GH, Liu B, Hong JS. Regional difference in susceptibility to lipopolysaccharide-induced neurotoxicity in the rat brain: role of microglia. *J Neurosci*. 2000; 20:6309–6316. [PubMed: 10934283]
3. Mittelbronn M, Dietz K, Schluesener HJ, Meyermann R. Local distribution of microglia in the normal adult human central nervous system differs by up to one order of magnitude. *Acta Neuropathol*. 2001; 101:249–255. [PubMed: 11307625]
4. Biber K, Neumann H, Inoue K, Boddeke HW. Neuronal ‘On’ and ‘Off’ signals control microglia. *Trends Neurosci*. 2007; 30:596–602. [PubMed: 17950926]
5. Domercq M, Vazquez-Villoldo N, Matute C. Neurotransmitter signaling in the pathophysiology of microglia. *Front Cell Neurosci*. 2013; 7:49. [PubMed: 23626522]
6. Brownstein MJ, Mroz EA, Kizer JS, Palkovits M, Leeman SE. Regional distribution of substance P in the brain of the rat. *Brain Res*. 1976; 116:299–305. [PubMed: 974776]
7. Kanazawa I, Mogaki S, Muramoto O, Kuzuhara S. On the origin of substance P-containing fibres in the entopeduncular nucleus and the substantia nigra of the rat. *Brain Res*. 1980; 184:481–485. [PubMed: 6153288]

8. Marriott I. The role of tachykinins in central nervous system inflammatory responses. *Front Biosci.* 2004; 9:2153–2165. [PubMed: 15353277]
9. Kowall NW, Quigley BJ Jr, Krause JE, Lu F, Kosofsky BE, Ferrante RJ. Substance P and substance P receptor histochemistry in human neurodegenerative diseases. *Regul Pept.* 1993; 46:174–185. [PubMed: 7692486]
10. Wang Q, Chu CH, Qian L, Chen SH, Wilson B, Oyarzabal E, Jiang L, Ali S, Robinson B, Kim HC, Hong JS. Substance P Exacerbates Dopaminergic Neurodegeneration through Neurokinin-1 Receptor-Independent Activation of Microglial NADPH Oxidase. *J Neurosci.* 2014; 34:12490–12503. [PubMed: 25209287]
11. Carolan EJ, Casale TB. Effects of neuropeptides on neutrophil migration through noncellular and endothelial barriers. *J Allergy Clin Immunol.* 1993; 92:589–598. [PubMed: 7691915]
12. Chernova I, Lai JP, Li H, Schwartz L, Tuluc F, Korchak HM, Douglas SD, Kilpatrick LE. Substance P (SP) enhances CCL5-induced chemotaxis and intracellular signaling in human monocytes, which express the truncated neurokinin-1 receptor (NK1R). *J Leukoc Biol.* 2009; 85:154–164. [PubMed: 18835883]
13. Wang Q, Shin EJ, Nguyen XK, Li Q, Bach JH, Bing G, Kim WK, Kim HC, Hong JS. Endogenous dynorphin protects against neurotoxin-elicited nigrostriatal dopaminergic neuron damage and motor deficits in mice. *J Neuroinflammation.* 2012; 9:124. [PubMed: 22695044]
14. Yang TT, Lin C, Hsu CT, Wang TF, Ke FY, Kuo YM. Differential distribution and activation of microglia in the brain of male C57BL/6J mice. *Brain Struct Funct.* 2013; 218:1051–1060. [PubMed: 22886465]
15. Sharaf A, Krieglstein K, Spittau B. Distribution of microglia in the postnatal murine nigrostriatal system. *Cell Tissue Res.* 2013; 351:373–382. [PubMed: 23250575]
16. Baby N, Li Y, Ling EA, Lu J, Dheen ST. Runx1t1 (Runt-related transcription factor 1; translocated to, 1) epigenetically regulates the proliferation and nitric oxide production of microglia. *PLoS One.* 2014; 9:e89326. [PubMed: 24586690]
17. Chen SH, Oyarzabal EA, Hong JS. Preparation of rodent primary cultures for neuron-glia, mixed glia, enriched microglia, and reconstituted cultures with microglia. *Methods Mol Biol.* 2013; 1041:231–240. [PubMed: 23813383]
18. Qin L, Liu Y, Wang T, Wei SJ, Block ML, Wilson B, Liu B, Hong JS. NADPH oxidase mediates lipopolysaccharide-induced neurotoxicity and proinflammatory gene expression in activated microglia. *J Biol Chem.* 2004; 279:1415–1421. [PubMed: 14578353]
19. Wang Q, Zhou H, Gao H, Chen SH, Chu CH, Wilson B, Hong JS. Naloxone inhibits immune cell function by suppressing superoxide production through a direct interaction with gp91phox subunit of NADPH oxidase. *J Neuroinflammation.* 2012; 9:32. [PubMed: 22340895]
20. Qian L, Wei SJ, Zhang D, Hu X, Xu Z, Wilson B, El-Benna J, Hong JS, Flood PM. Potent anti-inflammatory and neuroprotective effects of TGF-beta1 are mediated through the inhibition of ERK and p47phox-Ser345 phosphorylation and translocation in microglia. *J Immunol.* 2008; 181:660–668. [PubMed: 18566433]
21. Wang Q, Chu CH, Oyarzabal E, Jiang L, Chen SH, Wilson B, Qian L, Hong JS. Subpicomolar diphenyleonium inhibits microglial NADPH oxidase with high specificity and shows great potential as a therapeutic agent for neurodegenerative diseases. *Glia.* 2014; 62:2034–2043. [PubMed: 25043383]
22. Rosso M, Munoz M, Berger M. The role of neurokinin-1 receptor in the microenvironment of inflammation and cancer. *Scientific World Journal.* 2012; 2012:381434. [PubMed: 22545017]
23. Sun J, Ramnath RD, Tamizhselvi R, Bhatia M. Role of protein kinase C and phosphoinositide 3-kinase-Akt in substance P-induced proinflammatory pathways in mouse macrophages. *FASEB J.* 2009; 23:997–1010. [PubMed: 19029199]
24. Ginhoux F, Greter M, Leboeuf M, Nandi S, See P, Gokhan S, Mehler MF, Conway SJ, Ng LG, Stanley ER, Samokhvalov IM, Merad M. Fate mapping analysis reveals that adult microglia derive from primitive macrophages. *Science.* 2010; 330:841–845. [PubMed: 20966214]
25. Harry GJ. Microglia during development and aging. *Pharmacol Ther.* 2013; 139:313–326. [PubMed: 23644076]

26. Harry GJ, Kraft AD. Microglia in the developing brain: a potential target with lifetime effects. *Neurotoxicology*. 2012; 33:191–206. [PubMed: 22322212]
27. Luan J, Furuta Y, Du J, Richmond A. Developmental expression of two CXC chemokines, MIP-2 and KC, and their receptors. *Cytokine*. 2001; 14:253–263. [PubMed: 11444905]
28. Mosher KI, Andres RH, Fukuhara T, Bieri G, Hasegawa-Moriyama M, He Y, Guzman R, Wyss-Coray T. Neural progenitor cells regulate microglia functions and activity. *Nat Neurosci*. 2012; 15:1485–1487. [PubMed: 23086334]
29. Metcalf D. The granulocyte-macrophage colony stimulating factors. *Cell*. 1985; 43:5–6. [PubMed: 3000606]
30. Wang Y, Szretter KJ, Vermi W, Gilfillan S, Rossini C, Cella M, Barrow AD, Diamond MS, Colonna M. IL-34 is a tissue-restricted ligand of CSF1R required for the development of Langerhans cells and microglia. *Nat Immunol*. 2012; 13:753–760. [PubMed: 22729249]
31. Sun J, Ramnath RD, Zhi L, Tamizhselvi R, Bhatia M. Substance P enhances NF-kappaB transactivation and chemokine response in murine macrophages via ERK1/2 and p38 MAPK signaling pathways. *Am J Physiol Cell Physiol*. 2008; 294:C1586–1596. [PubMed: 18434625]
32. Sun J, Ramnath RD, Bhatia M. Neuropeptide substance P upregulates chemokine and chemokine receptor expression in primary mouse neutrophils. *Am J Physiol Cell Physiol*. 2007; 293:696–704.
33. Banisadr G, Gosselin RD, Mechighel P, Kitabgi P, Rostene W, Parsadaniantz SM. Highly regionalized neuronal expression of monocyte chemoattractant protein-1 (MCP-1/CCL2) in rat brain: evidence for its colocalization with neurotransmitters and neuropeptides. *J Comp Neurol*. 2005; 489:275–292. [PubMed: 16025454]
34. Ganter S, Northoff H, Mannel D, Gebicke-Harter PJ. Growth control of cultured microglia. *J Neurosci Res*. 1992; 33:218–230. [PubMed: 1333539]
35. Liu B, Wang K, Gao HM, Mandavilli B, Wang JY, Hong JS. Molecular consequences of activated microglia in the brain: overactivation induces apoptosis. *J Neurochem*. 2001; 77:182–189. [PubMed: 11279274]
36. Liu X, Ma B, Malik AB, Tang H, Yang T, Sun B, Wang G, Minshall RD, Li Y, Zhao Y, Ye RD, Xu J. Bidirectional regulation of neutrophil migration by mitogen-activated protein kinases. *Nat Immunol*. 2012; 13:457–464. [PubMed: 22447027]
37. Lelli A, Gervais A, Colin C, Cheret C, Ruiz de Almodovar C, Carmeliet P, Krause KH, Boillee S, Mallat M. The NADPH oxidase Nox2 regulates VEGFR1/CSF-1R-mediated microglial chemotaxis and promotes early postnatal infiltration of phagocytes in the subventricular zone of the mouse cerebral cortex. *Glia*. 2013; 61:1542–1555. [PubMed: 23836548]
38. Bey EA, Xu B, Bhattacharjee A, Oldfield CM, Zhao X, Li Q, Subbulakshmi V, Feldman GM, Wientjes FB, Cathcart MK. Protein kinase C delta is required for p47phox phosphorylation and translocation in activated human monocytes. *J Immunol*. 2004; 173:5730–5738. [PubMed: 15494525]
39. Double KL. Neuronal vulnerability in Parkinson's disease. *Parkinsonism Relat Disord*. 2012; 18(Suppl 1):S52–54. [PubMed: 22166454]
40. Gao HM, Hong JS. Why neurodegenerative diseases are progressive: uncontrolled inflammation drives disease progression. *Trends Immunol*. 2008; 29:357–365. [PubMed: 18599350]
41. Reid MS, Herrera-Marschitz M, Hokfelt T, Lindfors N, Persson H, Ungerstedt U. Striatonigral GABA, dynorphin, substance P and neurokinin A modulation of nigrostriatal dopamine release: evidence for direct regulatory mechanisms. *Exp Brain Res*. 1990; 82:293–303. [PubMed: 1704847]
42. Graybiel AM. Neuropeptides in the basal ganglia. *Res Publ Assoc Res Nerv Ment Dis*. 1986; 64:135–161. [PubMed: 2425403]
43. Barker R. Substance P and Parkinson's disease: a causal relationship? *J Theor Biol*. 1986; 120:353–362. [PubMed: 2431225]
44. Sivam SP. Dopamine dependent decrease in enkephalin and substance P levels in basal ganglia regions of postmortem parkinsonian brains. *Neuropeptides*. 1991; 18:201–207. [PubMed: 1711165]

45. Gerfen CR, Engber TM, Mahan LC, Susel Z, Chase TN, Monsma FJ Jr, Sibley DR. D1 and D2 dopamine receptor-regulated gene expression of striatonigral and striatopallidal neurons. *Science*. 1990; 250:1429–1432. [PubMed: 2147780]
46. Thornton E, Vink R. Treatment with a substance P receptor antagonist is neuroprotective in the intrastriatal 6-hydroxydopamine model of early Parkinson's disease. *PLoS One*. 2012; 7:e34138. [PubMed: 22485158]
47. Liu GJ, Nagarajah R, Banati RB, Bennett MR. Glutamate induces directed chemotaxis of microglia. *Eur J Neurosci*. 2009; 29:1108–1118. [PubMed: 19302147]
48. Zhang M, Xu G, Liu W, Ni Y, Zhou W. Role of fractalkine/CX3CR1 interaction in light-induced photoreceptor degeneration through regulating retinal microglial activation and migration. *PLoS One*. 2012; 7:e35446. [PubMed: 22536384]
49. Qin L, Wu X, Block ML, Liu Y, Breese GR, Hong JS, Knapp DJ, Crews FT. Systemic LPS causes chronic neuroinflammation and progressive neurodegeneration. *Glia*. 2007; 55:453–462. [PubMed: 17203472]

CLINICAL PERSPECTIVES

We have reported that SP potentiates microglial activation in the SN, amplifying dopaminergic neurodegeneration in experimental mouse models of PD. The purpose of this study was to investigate whether SP could regulate nigral microglial density.

Our findings indicated that unlike WT controls, mice deficient in SP or NK1R exhibited reduced nigral microglial density. SP did not interfere with microglial proliferative capacity but induced chemotaxis through mechanisms involving NK1R and NOX2 activation. Moreover, inhibition of PKC δ inhibited SP/NK1R-induced NOX2 activation in microglia.

Our results suggest that SP was a partial regulator of nigral microglial density through chemotactic recruitment mechanism. Our study not only recognized SP as a neurogenic microglia-regulatory signal but also provided valuable insights on how neurogenic signals regulating microglial density. Furthermore, the disproportionately high density of microglia and potential SP itself in the SN contributes to the increased susceptibility of nigral dopaminergic neurons in PD, therefore, the development of pharmacological inhibitors of SP/NK1R or NOX2 signals might be a novel direction for PD therapy.

SUMMARY STATEMENT

1. Reduced number of nigral microglia was observed in postnatal developing substance P- and neurokinin 1 receptor-deficient mice.
2. Substance P failed to interfere with microglial proliferation but induced migration through a neurokinin 1 receptor/protein kinase C δ /NADPH oxidase pathway-dependent manner.

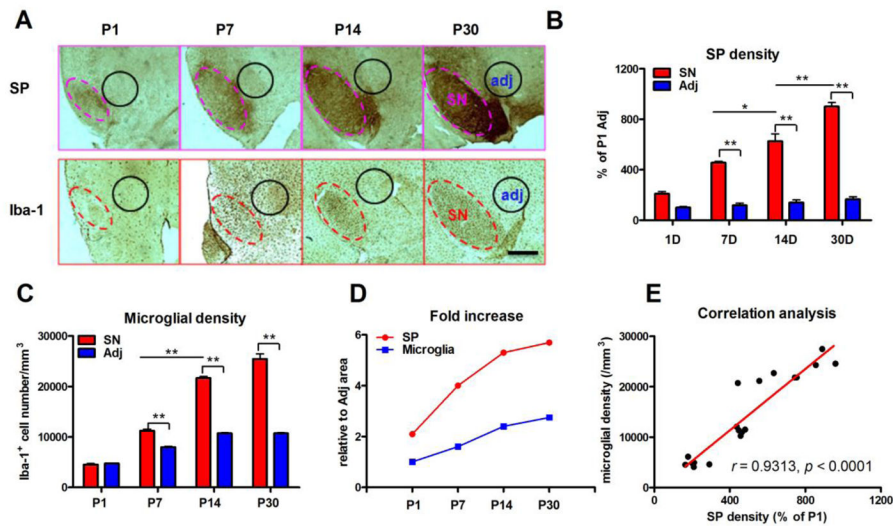


Figure 1. Time-dependent increase of densities of SP and microglia in the SN

(A) SP and microglia were stained with anti-SP and anti-Iba-1 antibody, respectively, in the SN at postnatal day 1 (P1), 7 (P7), 14 (P14) and 30 (P30) in C57BL/6 mice. (B) The densities of SP in the SN and adjacent area (as shown in A) were quantified by analyzing pixel density of SP staining using ImageJ. (C) Microglial density in the SN and adjacent area (as shown in A) was quantified by counting Iba-1-immunoreactive cells. A gradual increase of densities of SP and microglia in the SN was observed from P1 to P30. (D) Compared with adjacent area, fold increases of SP and microglial densities in the SN during postnatal development were calculated. (E) A positive correlation between increased expression of SP and microglial densities in the SN from P1 to P30 was observed. Results of microglial density are expressed as mean \pm SEM, while data of SP density are expressed as a percentage of P1 adjacent area (mean \pm SEM). * $p < 0.05$, ** $p < 0.01$. $n = 4-8$ in each group at each time point with total 18. Bar = 200 μm .

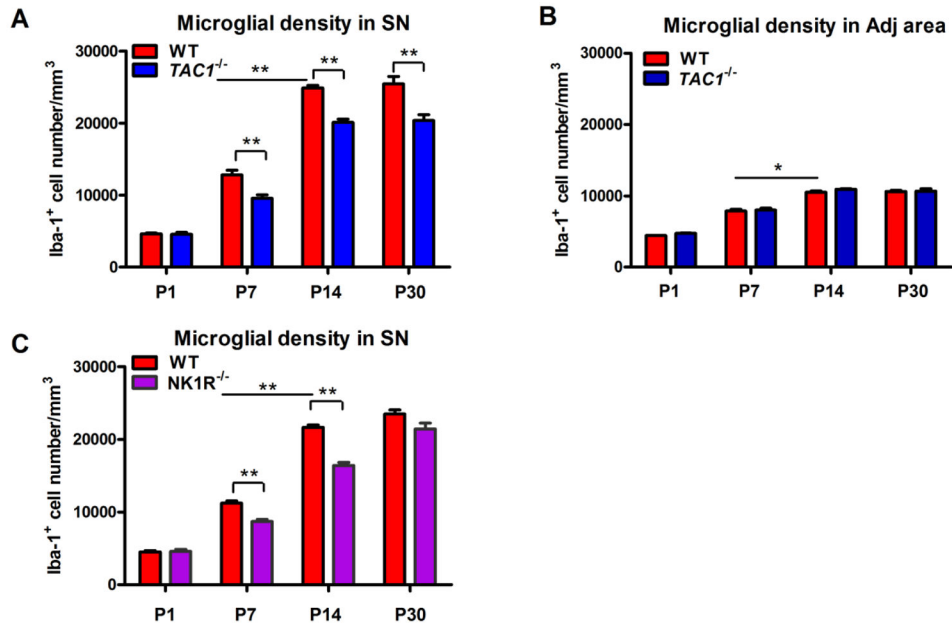


Figure 2. Lack of endogenous SP and NK1R decreases microglial density in the SN
 Microglia were stained with anti-Iba-1 antibody in the SN and its adjacent area of post-natal day 1 (P1), 7 (P7), 14 (P14) and 30 (P30) WT, *TAC1*^{-/-} and *NK1R*^{-/-} mice. (A–C) The density of microglia in the SN (A and C) and its adjacent area (B) was quantified by counting Iba-1-immunoreactive cells. Results are expressed as mean ± SEM. **p* < 0.05, ***p* < 0.01. *n* = 4–8 in each group at each time point with total 35, 18 and 18 for WT, *TAC1*^{-/-} and *NK1R*^{-/-} mice, respectively.

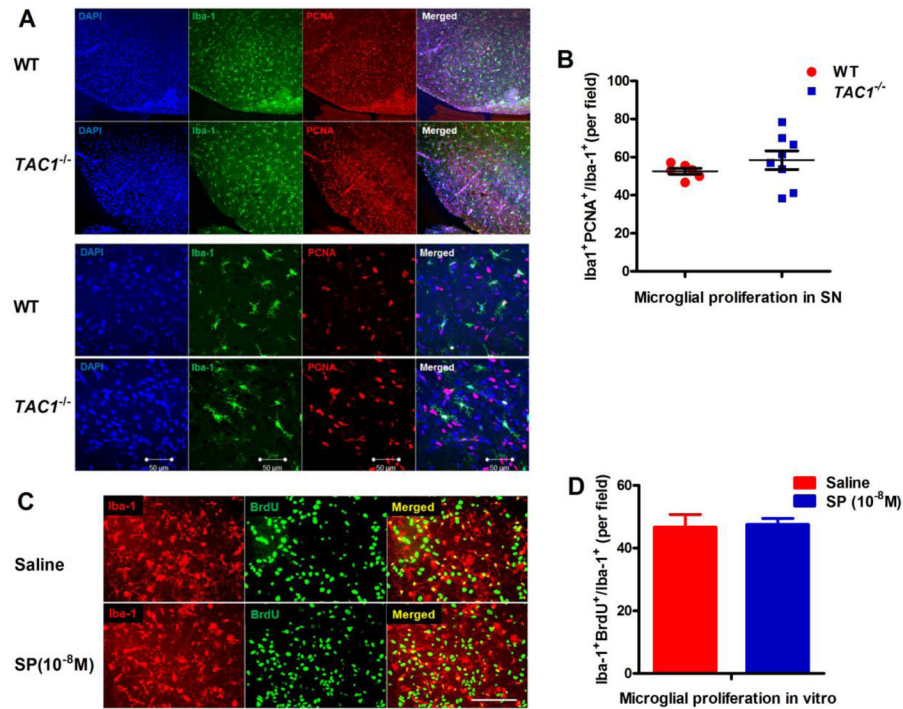


Figure 3. SP fails to affect microglial proliferative capacity

(A) Proliferating microglia were double stained with anti-Iba-1 and anti-PCNA antibodies in the SN of P7 WT and *TAC1*^{-/-} mice. Representative images in different magnifications were shown. (B) Iba-1⁺PCNA⁺ and Iba-1⁺ microglia were counted and the proliferative rate was calculated. n = 6 and 8 for WT and *TAC1*^{-/-} mice, respectively. (C) Mixed glia cultures were pre-incubated with BrdU (20 μmol/l) for 30 mins and followed by SP (10⁻⁸ M) or vehicle treatment for additional 72h. Proliferated microglia were recognized by double BrdU and Iba-1 immunoreactive cells. (D) The percentage of Iba-1⁺BrdU⁺ cells was calculated with respect to the total number of Iba-1⁺ cells. Results are expressed as mean ± SEM. n = 3. Bar = 50 μm.

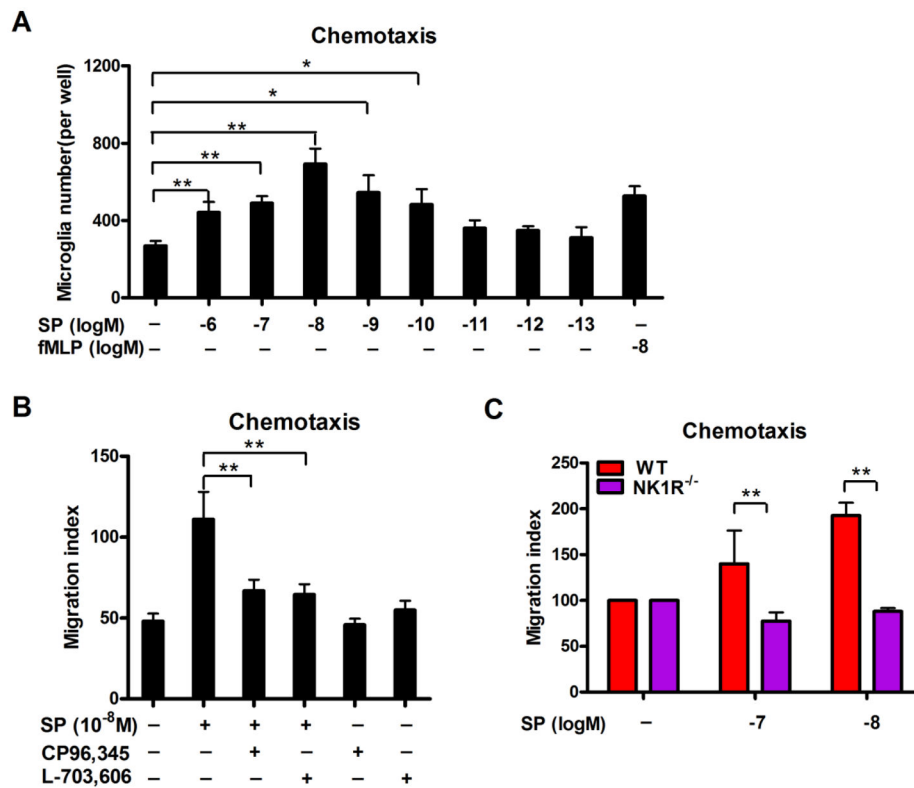


Figure 4. SP induces microglial migration in a trans-well system through a NK1R-dependent manner

(A) SP-induced microglial migration was assessed in a 96-well cell migration system with 5 μ m pore size using purified microglia. Different concentrations of SP (10^{-13} to 10^{-6} M) were placed in the bottom wells, and the number of microglia that migrated over the 4-hour incubation period was determined. fMLP (10^{-8} M) was served as a positive control. Data are expressed as mean \pm SEM. (B) Microglia were pre-treated with NK1R antagonist CP-96,345 or L-703,606 for 30 mins and followed by chemotaxis assay induced by 10^{-8} M SP. The number of migrated microglia was determined. (C) Purified microglia were prepared from WT and NK1R^{-/-} mice. The chemotaxis capacity of SP on WT and NK1R^{-/-} microglia was assessed. Results are expressed as the migration index (mean \pm SEM). * p < 0.05, ** p < 0.01. n = 4-5.

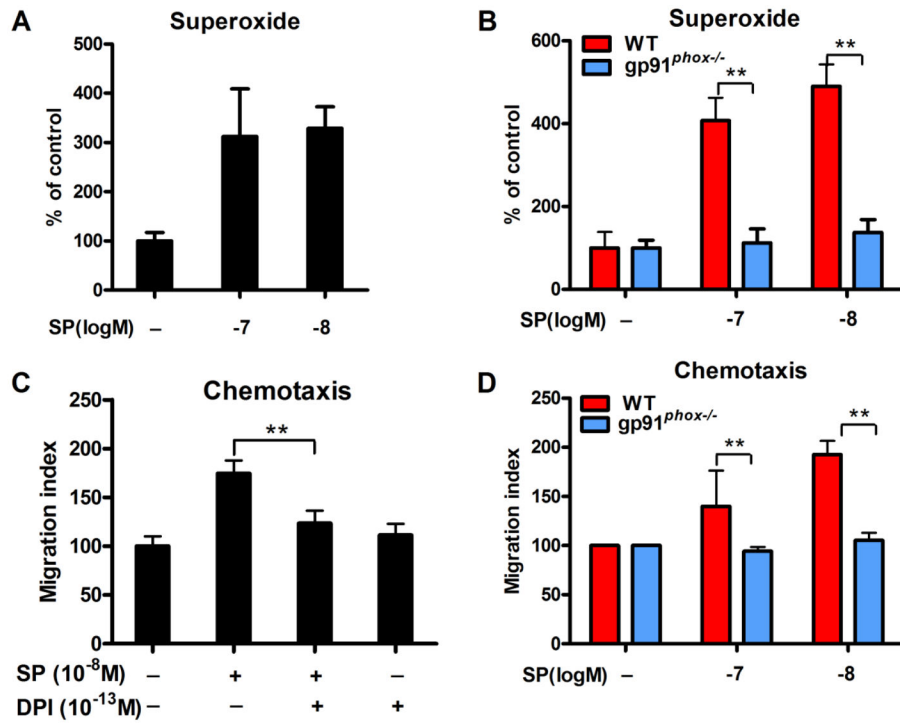


Figure 5. NOX2-generated superoxide is a critical mediator in SP-induced microglial chemotaxis (A) Mixed-glia cultures (containing 80% astroglia and 20% microglia) were treated with 10^{-7} or 10^{-8} M SP. Superoxide production was measured using SOD-inhibitable reduction of tetrazolium salt WST-1. (B) SP failed to produce superoxide in mix-glia cultures prepared from gp91^{phox-/-} mice. Data are expressed as the percentage of controls (mean \pm SEM). (C) Chemotaxis assay was performed by pre-treating microglia with NOX2 inhibitor DPI (10^{-13} M) for 30 mins and followed by SP (10^{-8} M) stimulation. (D) Purified microglia were prepared from WT and gp91^{phox-/-} mice. The chemotaxis capacity of SP on WT and gp91^{phox-/-} microglia was assessed. Results are expressed as the migration index (mean \pm SEM). * $p < 0.05$, ** $p < 0.01$. n = 4–5.

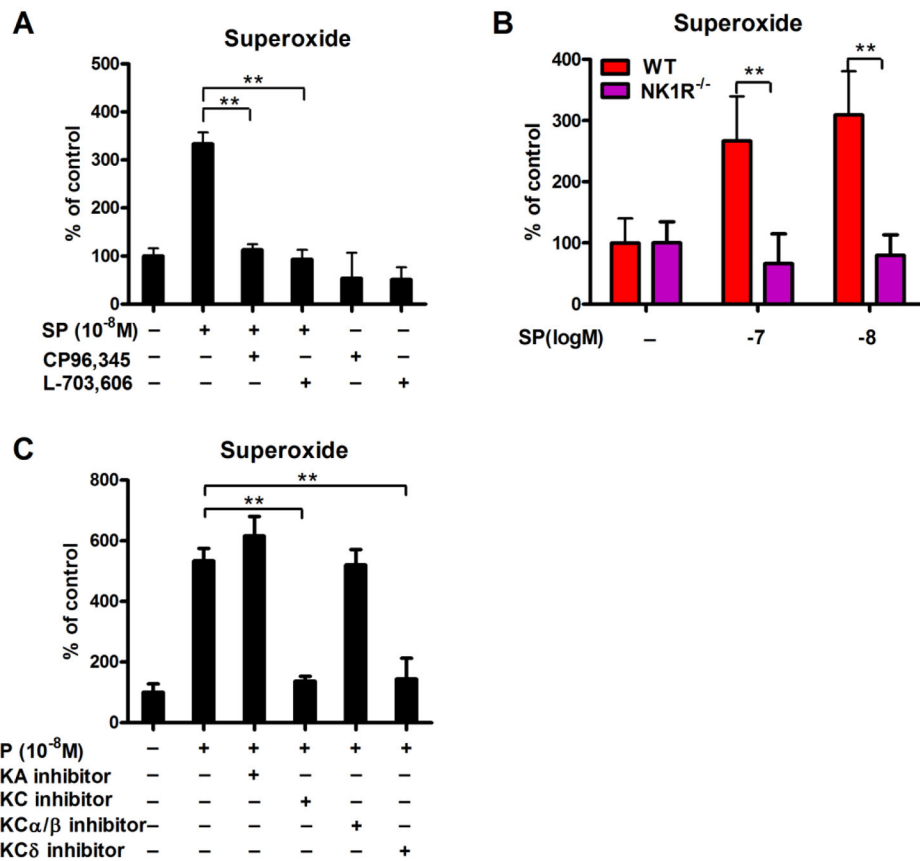


Figure 6. PKC δ bridges the cross-talk between NK1R and NOX2 in microglia induced by SP (A) Mixed-glia cultures were pre-treated with NK1R antagonists CP96,345 or L-703, 696 for 30 mins and followed by 10⁻⁸ M SP treatment. Superoxide production was measured using SOD-inhibitable reduction of tetrazolium salt WST-1. (B) The production of superoxide induced by SP was detected in mix-glia cells prepared from WT and NK1R^{-/-} mice. (C) Mix-glia cultures were pre-treated with inhibitors of PKA, PKC, PKC α/β or PKC δ for 30 mins, followed by SP (10⁻⁸ M) treatment. Superoxide production was measured. Results are expressed as the percentage of controls (mean \pm SEM). * p < 0.05, ** p < 0.01. n = 4–5.